

Simulations of Crystal Nucleation from Solution at Constant Chemical Potential

Tarak Karmakar^{†,‡}, Pablo M. Piaggi^{†,‡} and Michele Parrinello^{†,‡*}

[†]*Department of Chemistry and Applied Biosciences, ETH Zürich, c/o USI Campus, Via Giuseppe Buffi 13, CH-6900, Lugano, Ticino, Switzerland*

[‡]*Facoltà di Informatica, Istituto di Scienze Computazionali, Università della Svizzera Italiana (USI), Via Giuseppe Buffi 13, CH-6900, Lugano, Ticino, Switzerland.*

Received January 5, 2022; E-mail: michele.parrinello@phys.chem.ethz.ch

Abstract: A widely spread method of crystal preparation is to precipitate it from a supersaturated solution. In such a process, control of solution concentration is of paramount importance. Nucleation process, polymorph selection, and crystal habits depend crucially on this thermodynamic parameter. When performing simulations in the canonical ensemble as the crystalline phase is deposited the solution is depleted of solutes. This unavoidable modification of the thermodynamic conditions leads to significant artifact. Here we adopt the idea of the constant chemical potential molecular dynamics approach of Perego *et al.* [*J. Chem. Phys.* 2015, 142, 144113] to the study of nucleation. Our method allows determining the crystal nucleus size and nucleation rates at constant supersaturation. As an example we study the homogeneous nucleation of sodium chloride from its supersaturated aqueous solution.

1. INTRODUCTION

Crystal nucleation and growth from solution have great impact in chemical, material, biological, and environmental sciences. In solution, crystallization occurs by the aggregation of molecules or in general particles to form nuclei followed by their growth into macroscopic crystals. The early stage of this process contains valuable information on the microscopic pathways that lead to the formation of the crystal. However, unveiling such details of this deceptively simple process is a challenging task. Experiments have great difficulty in resolving the length and time scale of this process, and simulations have been proven to be of great help in this respect.¹⁻⁸

In crystallization from solution, supersaturation plays a crucial role in determining nucleation mechanisms⁹⁻¹³ and modulating polymorph selection.¹⁴⁻¹⁶ Thus it is important to study nucleation at constant solution supersaturation condition. However, modeling such a process on the computer is a non-trivial exercise. Computer simulations of nucleation from solution suffer from several limitations. One such limitation is the finite-size effect that arises while simulating nucleation in a small system with a fixed number of particles (typically a few thousands). During nucleation and growth, solute molecules are continuously drawn from the solution, and contrary to experiments, the finite-sized model system fails to retain a steady solution concentration in front of the growing nucleus. This solution depletion drastically affects further growth. Many remedies have been proposed to address this issue. Among them, the simplest one is to add an analytical correction term to the free energy profile.^{17,18} The other option is to simulate a considerably large system in which the finite-size effect is negligible.¹⁹ However, simulating a large system is often cumbersome. Alternatively, one could simulate an open system that can exchange particles with a fictitious external reservoir.²⁰ However, in many cases especially dense fluids, these methods encounter limitations due to low acceptance probabilities of particle insertion and deletion steps. Liu *et al.* proposed a string method in the osmotic ensemble to carry out constant supersaturation simulations.²¹

A more direct approach, called constant chemical potential molecular dynamics (C μ MD) has been recently introduced by Perego *et al.* in which the solution concentration in contact with a growing crystal slab is maintained at constant supersaturation leading to steady crystal growth.²² The C μ MD method²² and its cannibalistic variant²³ were used to investigate crystal growth and dissolution of organic molecules and active pharmaceuticals from solution at different supersaturations²⁴ and various solvents.²⁵

In the C μ MD approach, a slab geometry was adopted which was suitable for studying growth.²² However to study a nucleation process an isotropic model is more appropriate. Here, we present such a variant designed to carry out simulations of crystal nucleation from solution at constant supersaturation. In our method, a nucleus is grown inside a sphere, and the solution concentration inside a shell surrounding the sphere is maintained at a target concentration. We have applied our method to study the homogeneous nucleation of sodium chloride (NaCl) from aqueous solution at constant supersaturation. The reasons for the choice of this system are two-fold; first, it is a challenging multi-component system, and secondly, the availability of a substantial amount of simulation results²⁶⁻³³ makes it an

excellent system to test new methods.

2. COMPUTATIONAL METHODS

Constant Chemical Potential Simulation

In our C μ MD scheme, a sphere and a set of concentric shells are defined as shown schematically in Fig. 1. A spherical region of a fixed radius is selected from the simulation box center. This region is called the growth region (GR). The nucleus is grown in this region. The GR is chosen large enough to accommodate a nucleus larger than the critical nucleus size. A thin transition region (TR) shell is defined outside of the GR. A shell outside of the TR is defined by choosing inner and outer boundaries, r_{in} and r_{out} , respectively (Fig. 1). This shell is called the control region (CR). The solution concentration in this shell is maintained at a target concentration by an applied external force to be discussed later. The force-region (FR, yellow shell in Fig. 1) can be thought of as a membrane that allows solutes to enter/leave the CR depending on the concentration drop/increase in the CR. The region outside the FR serves as a molecular reservoir (buffer region) that, whenever needed, supplies solute atoms to the CR and thereby to the GR. The reservoir and the nested shells are periodically replicated, and periodic boundary conditions are imposed.

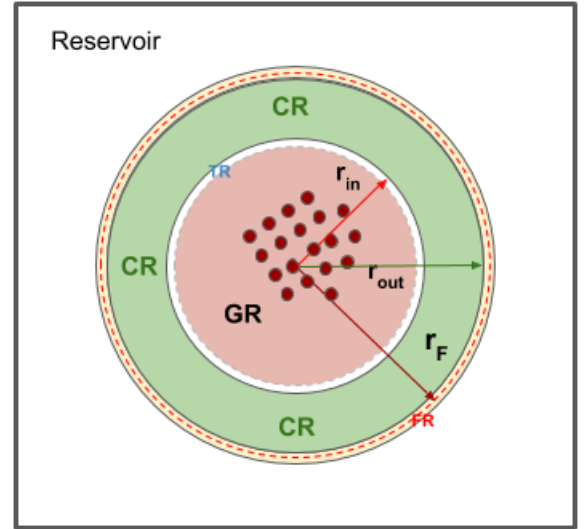


Figure 1. A two dimensional schematic description of the model system. The GR is shown in transparent red sphere. The white shell surrounding GR is the TR. The green shell is the CR. The force region (width w_F) is depicted by the yellow shell. The red dotted circle indicates the force center (r_F). A representative nucleus is shown in the GR by a cluster of red circles.

The solute concentration (c) in the CR is calculated as,

$$c = \frac{1}{V^{CR}} \sum_{j=1}^N f(r_j), \quad (1)$$

where V^{CR} is the CR volume and r_j the distance of a j -th particle from the box center. The $f(r_j)$ is a continuous and differentiable switching function that counts atoms belonging to the CR. In our case, this function is defined as a product of two Fermi switching functions, f_{in} (inward) and f_{out} (outward),

$$f(r_j) = f_{in}(r_j) \cdot f_{out}(r_j) = \frac{1}{1 + e^{-(r_j - r_{in})/\alpha}} \cdot \frac{1}{1 + e^{(r_j - r_{out})/\alpha}} \quad (2)$$

where, r_{in} and r_{out} are the inner and outer CR boundaries (Fig. 1), respectively, and α is a parameter that controls the switching functions steepness. The function $f(r_j)$ has a value of 1 when a solute is inside the CR and continuously approaches zero when outside. From now onward, we drop the atomic index for simplicity.

The force that restrains the instantaneous solution concentration (c in Eq. 1) at a target value (c_0) has the following expression,

$$F(r) = \kappa(c - c_0)G(r) \quad (3)$$

where κ is the force constant. The $G(r)$ in Eq. (3) is a bell-shaped function that localizes the $F(r)$ at r_F . This function is defined as,

$$G = \frac{1}{2\sigma} \left[\frac{1}{1 + \cosh(\frac{r-r_F}{\sigma})} \right] \quad (4)$$

where σ is a broadening parameter. Details of the C μ MD protocol and parameters used in our simulations are provided in Section 1 the SI.

Collective variables (CVs)

Crystal nucleation is a rare event that occurs on the time scale difficult to reach by regular atomistic simulations. Thanks to enhanced sampling simulation methods, we can circumvent the time scale limitation and study many long time-scale chemical and biophysical processes in short simulations at an affordable computational cost. One such enhanced sampling technique that has been used in many fields and demonstrated to be rigorous is metadynamics,^{34–36} especially in its well-tempered (WTMetaD) version.^{37,38} In this method, a history-dependent external bias is constructed as a function of a set of CVs that are a function of the atomic coordinates. Application of such a bias potential allows the system to transform from one state to another, which in the context of nucleation, are the solution without and with a crystal nucleus. In the following section, we provide details of the collective variables that we have used in the WTMetaD simulations. We introduce two CVs, one related to the local crystalline order and the other to the ionic solvation.

Local Order (CV₁)

The first CV is based on the local ordering of n neighbors (i) of a central atom in a crystal environment, χ . The local density $\rho_\chi(\mathbf{r})$ of the central atom is written as a sum of Gaussian functions,

$$\rho_\chi(\mathbf{r}) = \sum_{i \in \chi} e^{-|\mathbf{r}_i - \mathbf{r}|^2/2\sigma^2} \quad (5)$$

where \mathbf{r}_i 's are the coordinates of the neighbors relative to the central atom. σ^2 is the variance of the Gaussian functions. We now define a reference crystal environment (χ_0) and choose n nearest neighbors positions $\{\mathbf{r}_i^0\}$ of the central atom in the crystal lattice. The difference between the two environments χ and χ_0 is then calculated by a kernel function as done in ref. 39–41,

$$k_{\chi_0}(\chi) = \int d\mathbf{r} \rho_\chi(\mathbf{r}) \rho_{\chi_0}(\mathbf{r}) \quad (6)$$

where $\rho_{\chi_0}(\mathbf{r})$ is the local density of the atom in the reference crystal environment (χ_0). In ref 40, the reference environment is not fixed in space but rotated so as to obtain a rotationally invariant CV. Here we break the symmetry. In

doing so, the CV acquires a simple analytical expression.⁴¹

$$k_{\chi_0}(\chi) = \sum_{i \in \chi} \sum_{j \in \chi_0} \pi^{3/2} \sigma^3 e^{-|\mathbf{r}_i - \mathbf{r}_j|^2/4\sigma^2} \quad (7)$$

One shortcoming of this CV is that it can change its value by an overall rotation of the crystal. Since this is artificial, we add a restraint in order to avoid this unwanted effect (details can be found in SI).

The kernel function in Eq. (7) is then normalized such that similarities between the identical environments e.g., $\bar{k}_\chi(\chi)$ and $\bar{k}_{\chi_0}(\chi_0)$ are equal to one.

$$\begin{aligned} \bar{k}_{\chi_0}(\chi) &= \frac{k_\chi(\chi_0)}{k_{\chi_0}(\chi_0)} \\ &= \frac{1}{n} \sum_{i \in \chi} \sum_{j \in \chi_0} e^{-|\mathbf{r}_i - \mathbf{r}_j|^2/4\sigma^2} \end{aligned} \quad (8)$$

Now let us consider a system containing N solute particles. For each solute ($i = 1, \dots, N$) we calculate the kernel function $\bar{k}_{\chi_0}(\chi_i)$ using Eq. (8). The solutes having $\bar{k}_{\chi_0}(\chi_i) > k_0$, where $k_0=0.5$, are counted using a continuous and differentiable switching function (s_i^O) as follows,

$$s_i^O = \frac{1 - (\bar{k}_{\chi_0}(\chi_i)/k_0)^p}{1 - (\bar{k}_{\chi_0}(\chi_i)/k_0)^q} \quad (9)$$

The variable s_i^O has values in the range from 1 to 0; for crystalline atoms in a perfect environment, $s_i^O \approx 1$ while those in solution, $s_i^O \approx 0$. The s_i^O can be referred to as an atomic crystalline CV. Here the superscript O refers to the local order. The parameters p and q control the steepness and the range of the switching function.

The compound NaCl has a rock-salt crystal structure and the ions Na^+ and Cl^- form two interpenetrating FCC lattices. Each ion is surrounded by six of the oppositely charged ion arranged in an octahedral symmetry. We use one of these local environments as a reference structure. Here we have used as reference Na^+ and its Cl^- neighbors. However we could as well have used Cl^- as the central atom. A lattice parameter of 0.282 nm with $\sigma = 0.08$ nm was used for the kernel defined in Eq. (8).

Furthermore, since we were interested in biasing only the Na^+ ions inside the GR (Fig. 1), we used another switching function, $\omega(r_i)$ acting on the distance (r_i) between the s_i^O (Eq. 9) CVs position and the reference simulation box center, and to measure whether the s_i^O 's are inside the sphere or not. Finally, we define our first CV (s^O) as the sum over the crystalline Na^+ ions that are present inside the sphere,

$$s^O = \sum_i s_i^O \omega(r_i) \quad (10)$$

The switching function ($\omega(r_i)$) decays smoothly from 1 at a radius 1 nm to 0 beyond 1.5 nm from the box center.

Ion hydration (CV₂)

Solvent plays a pivotal role in the nucleation of ionic salts. During nucleation, increase in solute density is accompanied by ion dehydration; the latter is often found to be rate determining step.^{26,42–45} In aqueous solution, Na^+ and Cl^- ions are solvated with an average coordination number 6 and 8, respectively. In order to accelerate ions dehydration, we introduced another CV (s_i^H) which is based on water coordination number of each Na^+ ion ($i = 1, \dots, N$) within a given

cut-off radius (r_0),

$$s_i^H = \sum_j^{N_w} \frac{1 - (r_{ij}/r_0)^p}{1 - (r_{ij}/r_0)^q} \quad (11)$$

where, s_i^H is the water coordination number of i -th Na^+ ion, and r_{ij} and r_0 are the Na^+ - $\text{O}(\text{H}_2\text{O})$ distances and the distance cut-off, respectively. We have chosen $r_0=0.4$ nm in our case. N_w is the total number of water molecules in the system. The parameters p and q control the steepness of the switching function.

Finally, the second CV (s^H) is a weighted-average water-coordination number of Na^+ ions inside the sphere and defined as,

$$s^H = \frac{\sum_i s_i^H \omega(r_i)}{\sum_i \omega(r_i)} \quad (12)$$

In this case also, a cubic switching function ($\omega(r_i)$) is used. We drive explicitly Na^+ solvation. Adding the Cl^- solvation led to an increase in computational cost without much new insight.

It must be noted that by changing the geometry in Fig. 1 we cannot form infinitely repeated periodic crystals. For this reason we limit the size of the crystal that can be formed by imposing a restraint. We also found useful to put a limit to the number of waters that can solvate ions in order to avoid sampling configurations that are not relevant for the process under study.

System setup and simulation method

We considered a simulation box of dimension $\sim 6 \times 6 \times 6$ nm³. The box size was sufficient to accommodate the critical nucleus and a crystal in the growth region. The system contains 1000 ion-pairs (1000 Na^+ and 1000 Cl^-) and 6000 water molecules. The solution concentration is ~ 10 m (mole of solutes per kg of solvent). A similar concentration has been considered in previous studies to simulate NaCl nucleation from aqueous solution.^{27,31} The Juang-Cheatham force-field⁴⁶ was used to model the ions while water molecules were described with the SPC/E potential.⁴⁷ A time-step of 2 fs was employed. A cut-off of 0.9 nm was used for both van der Waals and short-range Coulomb interactions. The long-range electrostatic interactions were treated by the Particle Mesh Ewald method.⁴⁸ The enhanced sampling runs were started after equilibration run of 5 ns. During this initial phase the pressure was set at 1 bar using the Parrinello-Rahman barostat,⁴⁹ while the temperature was kept at 350 K using the stochastic velocity rescaling thermostat.⁵⁰ In the enhanced sampling runs that followed, we continued controlling the temperature with the same thermostat while the volume was kept constant thus switching to an (N,V,T) ensemble.

We have used the well-tempered metadynamics (WT-MetaD) method to carry out nucleation simulations. In the WTMetaD simulations, an initial hill height of 30 kJ/mol and widths of 0.5 and 0.1 for s^O and s^H , respectively were used. Hills were deposited every 500 steps. A bias factor of 100 and 50 were used.

All simulations were carried out using the GROMACS-2018.3 software patched with the PLUMED2 code. The C μ MD method and CV related codes are included in a private version of the PLUMED2 plugin. A representative PLUMED input file containing the CVs' information and the metadynamics protocol is provided in Section 2 (Fig. S1-4) of the SI. The visual Molecular Dynamics (VMD) soft-

ware⁵¹ was used to visualize the trajectories and produce some of the figures.

3. RESULTS AND DISCUSSION

After equilibration, we carried out three independent simulations (A, B, and C). In A, a standard NVT ensemble was used, and the initial value of the solution concentration was $c = 4.2$ nm⁻³. In B, the same concentration was imposed during the entire simulation run using the C μ MD method. In C, the concentration was kept at the higher value of $c = 5.0$ nm⁻³ using again the C μ MD approach. Contrasting A and B allows us studying the effect of keeping c constant, while from the difference between B and C the effect of increasing c can be investigated.

Let us start by discussing the results obtained from simulation A. When studying A even if not necessary, we use the CVs, s^O and s^H whose action is localized in a sphere of size 1.5 nm. This will allow a fairer comparison with a parallel C μ MD calculation. In order to understand the effect of nucleus growth on the solution concentration, we calculated its value in a shell 1.7 nm away from the box center and with a thickness of 0.8 nm. This region is the same as the one that is used in C μ MD simulations to monitor the solution concentration. During the metadynamics runs the concentration decreases as the size of the crystalline nucleus increases (see Fig. S6 of the SI). In contrast, in B and C, the instantaneous solution concentration fluctuates around the desired values (c_0) (Fig. S7). This accurate control of solution concentration demonstrates the effectiveness of our method.

Now that the solution concentration is well-controlled in all cases, we shift our attention toward the nucleation events. Metadynamics is able to induce multiple transitions to and from a NaCl microcrystal (Fig. 2(a) and Fig. S5). This enables us to collect enough statistics and calculate the free energy surfaces (FES). We followed a reweighting procedure discussed in ref. 52 to calculate the FESs as a function of s^O and $s^{H'}$ CVs. Here, $s^{H'}$ is defined as the number of Na^+ ions having less than 3 water molecules within radius 0.4 nm (see section 6 of the SI for details of the reweighting protocol). While the s^O reveals local ordering of the ions, $s^{H'}$ unveils the solvation effect. In Fig. 3(a) and 3(b), we can clearly see the effect of controlling c . In 3(a), the absence of a crystal minimum is to be noted. In contrast in 3(b), the crystal state appears as a local minimum. Increasing the solution concentration stabilizes the crystal phase (Fig. 3(c)). Furthermore, an almost straight diagonal path for the phase transition indicates that there is a single path for the transformation from the solution to the crystal state demonstrating that during nucleation ions crystallization and desolvation are correlated.

Additionally, we calculated one dimensional free energy profiles from the cluster size (n) distributions as described in ref. 53,54 and 55. The average free energy profiles and the errors were calculated using the block averaging analysis. The free energy profile obtained from simulation A (Fig. 4(a)) increases monotonously as the nucleus size increases. This could be due to the varying thermodynamical driving force induced by the solution depletion. In the B simulation, the free energy shows a barrier of 176 ± 28 kJ/mol, and after the critical nucleus, it decreases as the nucleus size increases. The lowering of the nucleation barrier in B simulation could be attributed to the controlled supersaturation

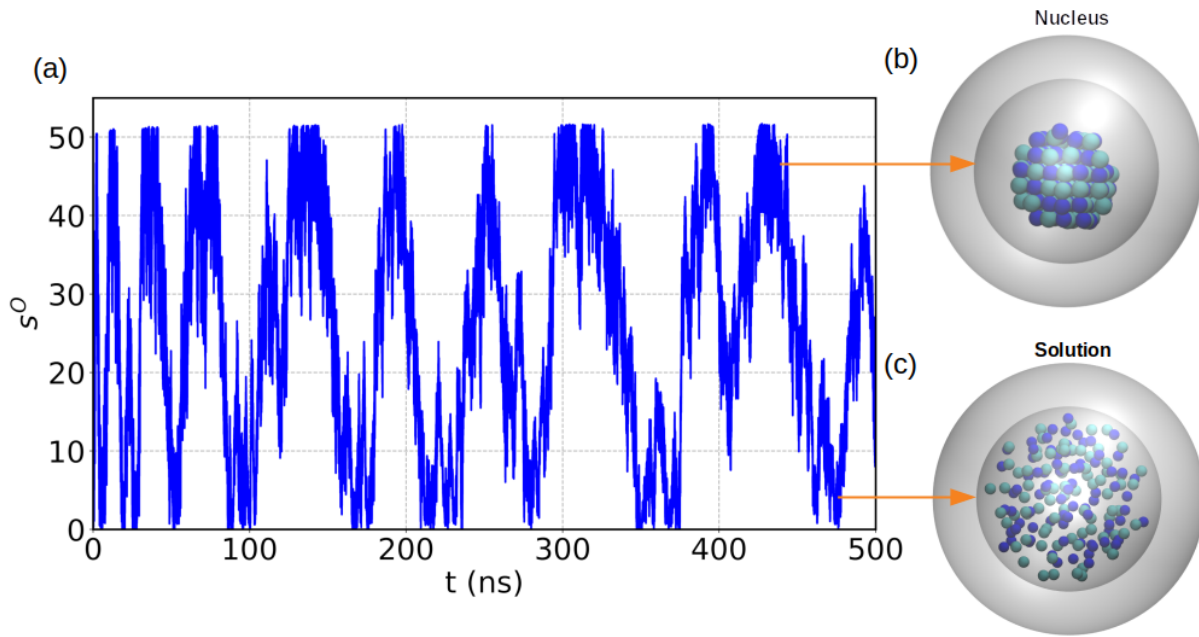


Figure 2. (a) The s^O CV plotted as a function of metadynamics simulation time (C simulation). The s^O and s^H profiles obtained from A and B simulations are provided in Fig. S5 of the SI. Representative frames extracted from two states, (b) a nucleus and (c) homogeneous solution in the GR. In (b), only the ions which are part of the nucleus are depicted in large spheres, and in both figures, other atoms in the whole system are not shown for clarity.

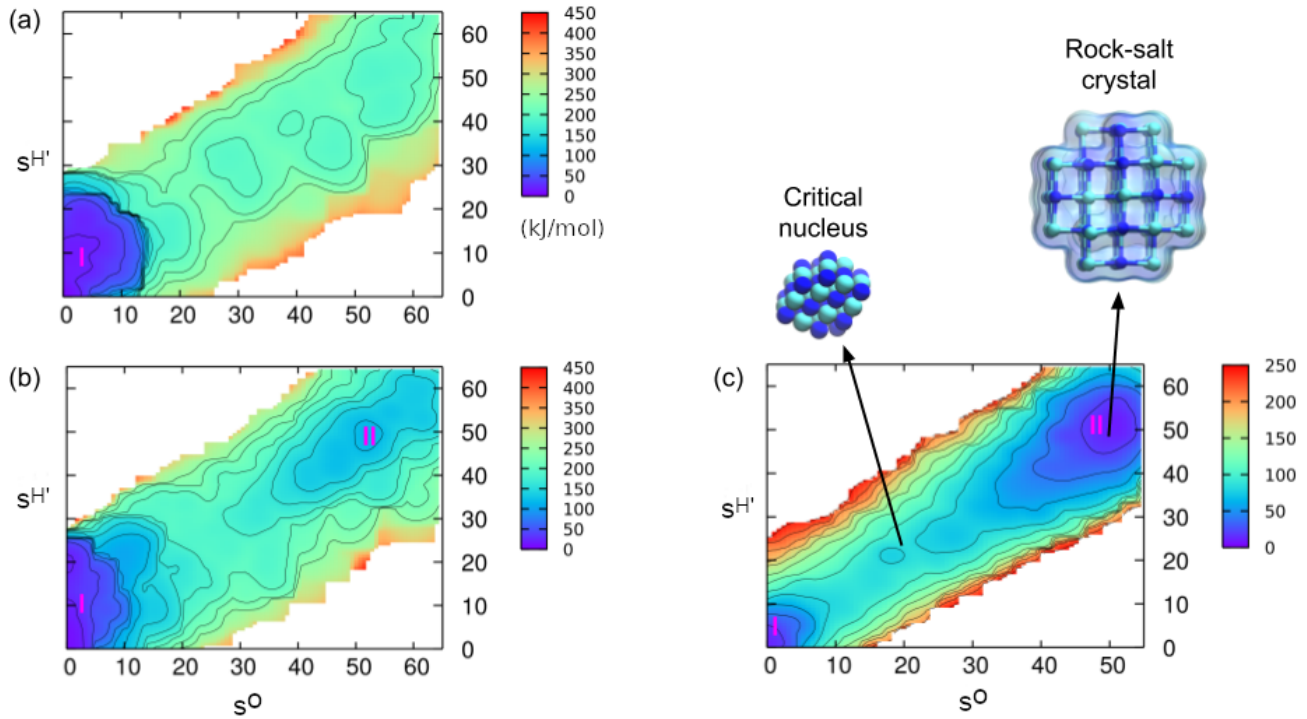


Figure 3. Free energy surfaces as a function of s^O and $s^{H'}$ obtained from the reweighting calculations on (a) A, (b) B, and (c) C simulation trajectories. The solution and the crystal basins on the FESs are marked by the symbols I and II, respectively. A representative critical nucleus and a rock-salt crystal collected from the crystal basin (from the C simulation trajectory) are presented.

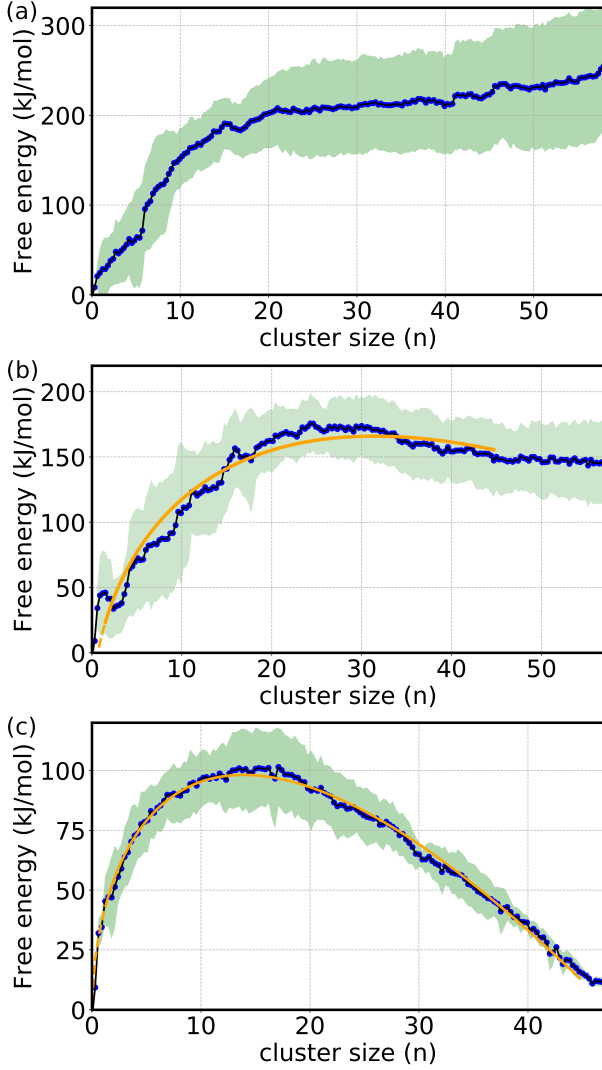


Figure 4. Reweighted one-dimensional free energy profiles as a function of cluster size (n) obtained from (a) A, (b) B, and (c) C simulations, respectively. To calculate the errors in the free energy profiles, blocks of 100 ns width (50-150, 100-200,..., 400-500) were selected from the 450 ns simulation trajectory (first 50 ns of the trajectory was discarded), and the free energy in each block was calculated. The average free energy profile is shown in blue spheres, and the standard deviations in green filled-region. The CNT-fitting curve is depicted in orange line.

condition. The critical nucleus (N_c) has been found to be comprised of approximately 27 ion-pairs. Furthermore, in the C simulation, with its increase in solution concentration, the free energy barrier decreases to 101 ± 10 kJ/mol. In this case, a smaller critical nucleus of size ~ 16 ion-pairs is obtained. The shape of these free energy curves (Fig 4(b) and (c)) spurred us to check if they fit to the classical nucleation theory (CNT) curve, and in fact, not surprisingly, a good fitting is obtained. The fitting of the free energy curve to the CNT-equation provided the chemical potential difference $\Delta\mu = 13.0$ kJ/mol for B and 13.8 kJ/mol for C simulation.

In the next step, following a protocol described in refs. 56–63 we calculate the nucleation rate (J)

$$J = \rho Z f^+ \exp(-\Delta F/k_B T) \quad (13)$$

where ρ is the number density, Z the Zeldovich factor,

f^+ the attachment frequency, ΔF the nucleation barrier, k_B the Boltzmann constant, and T the temperature. The $Z = \sqrt{|\Delta\mu|/6\pi k_B T N_c}$ is calculated using $\Delta\mu$ and N_c values. The attachment frequency (f^+) was obtained from the average slope of the $\langle (N - N_c)^2 \rangle$ vs. time curves obtained from a few short unbiased simulations initiated from configurations containing a critical nucleus (Fig. S11). All values related to the rate calculation are provided in Table S1 of the SI. Finally, we inserted all these values to the rate equation (Eq. 13) and obtain nucleation rates of $2.5 \times 10^3 \text{ cm}^{-3} \text{ s}^{-1}$ and $6.2 \times 10^{14} \text{ cm}^{-3} \text{ s}^{-1}$ at solution concentration $c = 4.2 \text{ nm}^{-3}$ and $c = 5.0 \text{ nm}^{-3}$, respectively, and at temperature 350 K. The unavailability of NaCl nucleation rate at high temperatures does not allow a direct comparison of our results with experiments. However, the obtained nucleation rates are close to the values ($10^1 - 10^{25} \text{ cm}^{-3} \text{ s}^{-1}$) at ambient conditions.^{29,31,64,65}

Although not the primary focus of our work, here we provide a summary of observations related to the nucleation mechanism gathered from the simulation trajectories. A visual inspection of the simulation trajectories reveals single-step nucleation mechanism. Moreover, the CNT-like free energy profile obtained from the $C\mu\text{MD}$ simulations depicted in Fig. 4(b) and (c) is an indicator of a likely one-step nucleation mechanism. Our observations are in line with the previous reports.^{31,32} Furthermore, in our simulations, we do not observe the Wurtzite structure reported in a few studies.^{27,66} This could be due to the choice of our CV which only describes the rock-salt structure. A movie demonstrating a representative nucleation event extracted from the C simulation is provided as a web-enhanced SI.

4. CONCLUSION

In summary, we have developed a $C\mu\text{MD}$ simulation method to carry out simulation of nucleation from solution at constant chemical potential. The presented method has been demonstrated to be effective in controlling the solution supersaturation surrounding the growing embryo leads to steady nucleation. Although in this particular case, the solution depletion is not severe ($\sim 7\text{-}10\%$), it could be more significant when a large crystal is grown from solution in a closed finite-size system.

An effective chemical potential control together with metadynamics simulations helped us in calculating NaCl nucleation free energy surfaces at a given solution concentration. The local order-based collective variable (s^O) employed in our metadynamics simulations has been found to be delicate in growing a target crystal structure. A single pathway for the transformation from the solution to the crystal has been realized. The CNT-like free energy curve further confirms that NaCl follows a single-step nucleation in supersaturated aqueous solution.

The $C\mu\text{MD}$ method introduced here opens up many possible applications. An immediate application would be to carry out seeded nucleation at constant solution concentration. Alternatively one can interface our method with several enhanced sampling methods^{67,68} focusing nucleation e.g., forward-flux sampling,⁶⁹ persistent-embryo approach,⁷⁰ and string method^{21,71,72} to carry out controlled nucleation at constant solution concentration. Furthermore, multi-resolution scheme such as adaptive resolution^{73–80} can also be combined with the presented $C\mu\text{MD}$ technique to

carry out concentration-controlled nucleation simulations of a system with a relatively large reservoir containing low-resolution coarse-grain solute and solvents.

The method is no way limited to the study of nucleation but could be useful in simulating controlled self-assembly of small organic and biomolecules such as peptides. We believe the realistic nature of our method in mimicking bulk-like environment to the growing nucleus or cluster will help in obtaining true kinetics.

5. ASSOCIATED CONTENT

Supporting Information

The supporting information contains C μ MD protocol, sample PLUMED input files, details of the restraints used in metadynamics simulations, time series of s^O and s^H CVs for A, B, and C simulations, a correlation plot of solution concentration and s^O CV from A simulation, solution concentration profiles obtained from simulations B and C, time evolution of mean square change in the cluster size, a table containing values related to rate calculations.

A movie demonstrating a nucleation event can be found here ()

The codes used in this work are included in the private development version of PLUMED2 plugin and will be openly available in the future. Until the official release, the codes will be available upon request to the corresponding authors.

6. AUTHOR INFORMATION

Corresponding Author*

E-mail: michele.parrinello@phys.chem.ethz.ch

ORCID:

Tarak Karmakar: 0000-0002-8721-6247

Michele Parrinello: 0000-0001-6550-3272

Present Address

[†]Department of Chemistry and Applied Biosciences, ETH Zurich, c/o USI Campus, Via Giuseppe Buffi 13, CH-6900, Lugano, Ticino, Switzerland

[‡]Facoltà di Informatica, Istituto di Scienze Computazionali, Università della Svizzera Italiana (USI), Via Giuseppe Buffi 13, CH-6900, Lugano, Ticino, Switzerland.

Notes:

The authors declare no competing financial interest.

7. ACKNOWLEDGEMENTS

The authors would like to thank Luigi Bonati, Michele Invernizzi, Dr. Haiyang Niu, and Jayashrita Debnath for providing useful suggestions. We thank CSCS, Swiss National Supercomputing Centre for providing the computational resources. The research was supported by the European Union Grant No. ERC-2014-AdG-670227/VARMET. We also acknowledge the NCCR MARVEL, funded by the Swiss National Science Foundation.

References

- (1) Ohtaki, H.; Fukushima, N. Nucleation processes of NaCl and CsF crystals from aqueous solutions studied by molecular dynamics simulations. *Pure and applied chemistry* **1991**, *63*, 1743–1748.
- (2) Anwar, J.; Boateng, P. K. Computer simulation of crystallization from solution. *Journal of the American Chemical Society* **1998**, *120*, 9600–9604.
- (3) Shore, J. D.; Perchak, D.; Shnidman, Y. Simulations of the nucleation of AgBr from solution. *The Journal of Chemical Physics* **2000**, *113*, 6276–6284.
- (4) Sarupria, S.; Debenedetti, P. G. Homogeneous nucleation of methane hydrate in microsecond molecular dynamics simulations. *The journal of physical chemistry letters* **2012**, *3*, 2942–2947.
- (5) Salvalaglio, M.; Perego, C.; Giberti, F.; Mazzotti, M.; Parrinello, M. Molecular-dynamics simulations of urea nucleation from aqueous solution. *Proceedings of the National Academy of Sciences* **2015**, *112*, E6–E14.
- (6) Sosso, G. C.; Chen, J.; Cox, S. J.; Fitzner, M.; Pedevilla, P.; Zen, A.; Michaelides, A. Crystal nucleation in liquids: Open questions and future challenges in molecular dynamics simulations. *Chemical reviews* **2016**, *116*, 7078–7116.
- (7) Fitzner, M.; Sosso, G. C.; Pietrucci, F.; Pipolo, S.; Michaelides, A. Pre-critical fluctuations and what they disclose about heterogeneous crystal nucleation. *Nature communications* **2017**, *8*, 2257.
- (8) Sosso, G. C.; Whale, T. F.; Holden, M. A.; Pedevilla, P.; Murray, B. J.; Michaelides, A. Unravelling the origins of ice nucleation on organic crystals. *Chemical science* **2018**, *9*, 8077–8088.
- (9) Vekilov, P. G. The two-step mechanism of nucleation of crystals in solution. *Nanoscale* **2010**, *2*, 2346–2357.
- (10) Myerson, A. S.; Trout, B. L. Nucleation from solution. *Science* **2013**, *341*, 855–856.
- (11) De Yoreo, J. Crystal nucleation: more than one pathway. *Nature materials* **2013**, *12*, 284.
- (12) Tan, W.; Yang, X.; Duan, X.; Zhang, X.; Qian, G.; Zhou, X. Understanding supersaturation-dependent crystal growth of L-alanine in aqueous solution. *Crystal Research and Technology* **2016**, *51*, 23–29.
- (13) Lee, S.; Wi, H. S.; Jo, W.; Cho, Y. C.; Lee, H. H.; Jeong, S.-Y.; Kim, Y.-I.; Lee, G. W. Multiple pathways of crystal nucleation in an extremely supersaturated aqueous potassium dihydrogen phosphate (KDP) solution droplet. *Proceedings of the National Academy of Sciences* **2016**, *113*, 13618–13623.
- (14) Sudha, C.; Srinivasan, K. Supersaturation dependent nucleation control and separation of mono, ortho and unstable polymorphs of paracetamol by swift cooling crystallization technique. *CrystEngComm* **2013**, *15*, 1914–1921.
- (15) Liang, S.; Duan, X.; Zhang, X.; Qian, G.; Zhou, X. Supersaturation-dependent polymorphic outcome and transformation rate of L-glutamic acid. *RSC Advances* **2016**, *6*, 74700–74703.
- (16) Liu, Y.; van den Berg, M. H.; Alexander, A. J. Supersaturation dependence of glycine polymorphism using laser-induced nucleation, sonocrystallization and nucleation by mechanical shock. *Physical Chemistry Chemical Physics* **2017**, *19*, 19386–19392.
- (17) Salvalaglio, M.; Vetter, T.; Giberti, F.; Mazzotti, M.; Parrinello, M. Uncovering molecular details of urea crystal growth in the presence of additives. *Journal of the American Chemical Society* **2012**, *134*, 17221–17233.
- (18) Agarwal, V.; Peters, B. Nucleation near the eutectic point in a Potts-lattice gas model. *The Journal of chemical physics* **2014**, *140*, 084111.
- (19) Wedekind, J.; Reguera, D.; Strey, R. Finite-size effects in simulations of nucleation. *The Journal of chemical physics* **2006**, *125*, 214505.
- (20) Horsch, M.; Vrabec, J. Grand canonical steady-state simulation of nucleation. *The Journal of chemical physics* **2009**, *131*, 184104.
- (21) Liu, C.; Wood, G. P.; Santiso, E. E. Modelling nucleation from solution with the string method in the osmotic ensemble. *Molecular Physics* **2018**, *116*, 2998–3007.
- (22) Perego, C.; Salvalaglio, M.; Parrinello, M. Molecular dynamics simulations of solutions at constant chemical potential. *The Journal of chemical physics* **2015**, *142*, 144113.
- (23) Karmakar, T.; Piaggi, P. M.; Perego, C.; Parrinello, M. A Cannibalistic Approach to Grand Canonical Crystal Growth. *Journal of chemical theory and computation* **2018**, *14*, 2678–2683.
- (24) Bjelobrk, Z.; Piaggi, P. M.; Weber, T.; Karmakar, T.; Mazzotti, M.; Parrinello, M. Naphthalene crystal shape prediction from molecular dynamics simulations. *CrystEngComm* **2019**.
- (25) Han, D.; Karmakar, T.; Bjelobrk, Z.; Gong, J.; Parrinello, M. Solvent-mediated morphology selection of the active pharmaceutical ingredient isoniazid: Experimental and simulation studies. *Chemical Engineering Science* **2018**.
- (26) Zahn, D. Atomistic mechanism of NaCl nucleation from an aqueous solution. *Physical review letters* **2004**, *92*, 040801.
- (27) Zimmermann, N. E.; Vorselaars, B.; Quigley, D.; Peters, B. Nucleation of NaCl from aqueous solution: Critical sizes, ion-attachment kinetics, and rates. *Journal of the American Chem-*

- ical Society **2015**, *137*, 13352–13361.
- (28) Lanaro, G.; Patey, G. Birth of NaCl crystals: Insights from molecular simulations. *The Journal of Physical Chemistry B* **2016**, *120*, 9076–9087.
 - (29) Zimmermann, N. E.; Vorselaars, B.; Espinosa, J. R.; Quigley, D.; Smith, W. R.; Sanz, E.; Vega, C.; Peters, B. NaCl nucleation from brine in seeded simulations: Sources of uncertainty in rate estimates. *The Journal of chemical physics* **2018**, *148*, 222838.
 - (30) Jiang, H.; Debenedetti, P. G.; Panagiotopoulos, A. Z. Communication: Nucleation rates of supersaturated aqueous NaCl using a polarizable force field. *The Journal of chemical physics* **2018**, *149*, 141102.
 - (31) Jiang, H.; Haji-Akbari, A.; Debenedetti, P. G.; Panagiotopoulos, A. Z. Forward flux sampling calculation of homogeneous nucleation rates from aqueous NaCl solutions. *The Journal of chemical physics* **2018**, *148*, 044505.
 - (32) Jiang, H.; Debenedetti, P. G.; Panagiotopoulos, A. Z. Nucleation in aqueous NaCl solutions shifts from 1-step to 2-step mechanism on crossing the spinodal. *The Journal of Chemical Physics* **2019**, *150*, 124502.
 - (33) Patel, L. A.; Kindt, J. T. Simulations of NaCl Aggregation from Solution: Solvent Determines Topography of Free Energy Landscape. *Journal of computational chemistry* **2019**, *40*, 135–147.
 - (34) Laio, A.; Parrinello, M. Escaping free-energy minima. *Proceedings of the National Academy of Sciences* **2002**, *99*, 12562–12566.
 - (35) Laio, A.; Gervasio, F. L. Metadynamics: a method to simulate rare events and reconstruct the free energy in biophysics, chemistry and material science. *Reports on Progress in Physics* **2008**, *71*, 126601.
 - (36) Barducci, A.; Bonomi, M.; Parrinello, M. Metadynamics. *Wiley Interdisciplinary Reviews: Computational Molecular Science* **2011**, *1*, 826–843.
 - (37) Barducci, A.; Bussi, G.; Parrinello, M. Well-tempered metadynamics: A smoothly converging and tunable free-energy method. *Phys. Rev. Lett.* **2008**, *100*, 020603.
 - (38) Dama, J. F.; Parrinello, M.; Voth, G. A. Well-tempered metadynamics converges asymptotically. *Physical review letters* **2014**, *112*, 240602.
 - (39) Bartók, A. P.; Kondor, R.; Csányi, G. On representing chemical environments. *Physical Review B* **2013**, *87*, 184115.
 - (40) De, S.; Bartók, A. P.; Csányi, G.; Ceriotti, M. Comparing molecules and solids across structural and alchemical space. *Physical Chemistry Chemical Physics* **2016**, *18*, 13754–13769.
 - (41) Piaggi, P. M.; Parrinello, M. Phase diagrams from single molecular dynamics simulations. *The Journal of Chemical Physics* **2019**, *150*, 244119.
 - (42) Piana, S.; Jones, F.; Gale, J. D. Assisted desolvation as a key kinetic step for crystal growth. *Journal of the American Chemical Society* **2006**, *128*, 13568–13574.
 - (43) Kowacz, M.; Putnis, C.; Putnis, A. The effect of cation: anion ratio in solution on the mechanism of barite growth at constant supersaturation: role of the desolvation process on the growth kinetics. *Geochimica et Cosmochimica Acta* **2007**, *71*, 5168–5179.
 - (44) Raiteri, P.; Gale, J. D. Water is the key to nonclassical nucleation of amorphous calcium carbonate. *Journal of the American Chemical Society* **2010**, *132*, 17623–17634.
 - (45) Joswiak, M. N.; Doherty, M. F.; Peters, B. Ion dissolution mechanism and kinetics at kink sites on NaCl surfaces. *Proceedings of the National Academy of Sciences* **2018**, *115*, 656–661.
 - (46) Joung, I. S.; Cheatham III, T. E. Molecular dynamics simulations of the dynamic and energetic properties of alkali and halide ions using water-model-specific ion parameters. *The Journal of Physical Chemistry B* **2009**, *113*, 13279–13290.
 - (47) Berendsen, H.; Grigera, J.; Straatsma, T. The missing term in effective pair potentials. *Journal of Physical Chemistry* **1987**, *91*, 6269–6271.
 - (48) Essmann, U.; Perera, L.; Berkowitz, M. L.; Darden, T.; Lee, H.; Pedersen, L. G. A smooth particle mesh Ewald method. *The Journal of chemical physics* **1995**, *103*, 8577–8593.
 - (49) Parrinello, M.; Rahman, A. Polymorphic transitions in single crystals: A new molecular dynamics method. *J. Appl. Phys.* **1981**, *52*, 7182–7190.
 - (50) Bussi, G.; Donadio, D.; Parrinello, M. Canonical sampling through velocity rescaling. *The Journal of chemical physics* **2007**, *126*, 014101.
 - (51) Humphrey, W.; Dalke, A.; Schulten, K. VMD: visual molecular dynamics. *Journal of molecular graphics* **1996**, *14*, 33–38.
 - (52) Tiwary, P.; Parrinello, M. A time-independent free energy estimator for metadynamics. *The Journal of Physical Chemistry B* **2014**, *119*, 736–742.
 - (53) Piaggi, P. M.; Valsson, O.; Parrinello, M. A variational approach to nucleation simulation. *Faraday discussions* **2017**, *195*, 557–568.
 - (54) Niu, H.; Piaggi, P. M.; Invernizzi, M.; Parrinello, M. Molecular dynamics simulations of liquid silica crystallization. *Proceedings of the National Academy of Sciences* **2018**, *115*, 5348–5352.
 - (55) Niu, H.; Yang, Y. I.; Parrinello, M. Temperature Dependence of Homogeneous Nucleation in Ice. *Physical Review Letters* **2019**, *122*, 245501.
 - (56) Becker, R.; Döring, W. Kinetische behandlung der keimbildung in übersättigten dämpfen. *Annalen der Physik* **1935**, *416*, 719–752.
 - (57) Auer, S.; Frenkel, D. Prediction of absolute crystal-nucleation rate in hard-sphere colloids. *Nature* **2001**, *409*, 1020.
 - (58) Lundrigan, S. E.; Saika-Voivod, I. Test of classical nucleation theory and mean first-passage time formalism on crystallization in the Lennard-Jones liquid. *The Journal of Chemical Physics* **2009**, *131*, 104503.
 - (59) Sanz, E.; Vega, C.; Espinosa, J.; Caballero-Bernal, R.; Abascal, J.; Valeriani, C. Homogeneous ice nucleation at moderate supercooling from molecular simulation. *Journal of the American Chemical Society* **2013**, *135*, 15008–15017.
 - (60) Espinosa, J.; Navarro, C.; Sanz, E.; Valeriani, C.; Vega, C. On the time required to freeze water. *The Journal of chemical physics* **2016**, *145*, 211922.
 - (61) Espinosa, J. R.; Vega, C.; Valeriani, C.; Sanz, E. Seeding approach to crystal nucleation. *The Journal of chemical physics* **2016**, *144*, 034501.
 - (62) Espinosa, J.; Sanz, E.; Valeriani, C.; Vega, C. Homogeneous ice nucleation evaluated for several water models. *The Journal of chemical physics* **2014**, *141*, 18C529.
 - (63) Soria, G. D.; Espinosa, J. R.; Ramirez, J.; Valeriani, C.; Vega, C.; Sanz, E. A simulation study of homogeneous ice nucleation in supercooled salty water. *The Journal of chemical physics* **2018**, *148*, 222811.
 - (64) Na, H.-S.; Arnold, S.; Myerson, A. S. Cluster formation in highly supersaturated solution droplets. *Journal of crystal growth* **1994**, *139*, 104–112.
 - (65) Gao, Y.; Yu, L. E.; Chen, S. B. Efflorescence relative humidity of mixed sodium chloride and sodium sulfate particles. *The Journal of Physical Chemistry A* **2007**, *111*, 10660–10666.
 - (66) Giberti, F.; Tribello, G. A.; Parrinello, M. Transient polymorphism in NaCl. *Journal of chemical theory and computation* **2013**, *9*, 2526–2530.
 - (67) Fillion, L.; Hermes, M.; Ni, R.; Dijkstra, M. Crystal nucleation of hard spheres using molecular dynamics, umbrella sampling, and forward flux sampling: A comparison of simulation techniques. *The Journal of chemical physics* **2010**, *133*, 244115.
 - (68) Weinan, E.; Vanden-Eijnden, E. Transition-path theory and path-finding algorithms for the study of rare events. *Annual review of physical chemistry* **2010**, *61*, 391–420.
 - (69) Allen, R. J.; Valeriani, C.; ten Wolde, P. R. Forward flux sampling for rare event simulations. *Journal of physics: Condensed matter* **2009**, *21*, 463102.
 - (70) Sun, Y.; Song, H.; Zhang, F.; Yang, L.; Ye, Z.; Mendelev, M. I.; Wang, C.-Z.; Ho, K.-M. Overcoming the time limitation in Molecular Dynamics simulation of crystal nucleation: a persistent-embryo approach. *Physical review letters* **2018**, *120*, 085703.
 - (71) Weinan, E.; Ren, W.; Vanden-Eijnden, E. Finite temperature string method for the study of rare events. *J. Phys. Chem. B* **2005**, *109*, 6688–6693.
 - (72) Maragliano, L.; Fischer, A.; Vanden-Eijnden, E.; Cicciotti, G. String method in collective variables: Minimum free energy paths and isocommittor surfaces. *The Journal of chemical physics* **2006**, *125*, 024106.
 - (73) Praprotnik, M.; Site, L. D.; Kremer, K. Multiscale simulation of soft matter: From scale bridging to adaptive resolution. *Annu. Rev. Phys. Chem.* **2008**, *59*, 545–571.
 - (74) Praprotnik, M.; Delle Site, L.; Kremer, K. Adaptive resolution molecular-dynamics simulation: Changing the degrees of freedom on the fly. *The Journal of chemical physics* **2005**, *123*, 224106.
 - (75) Praprotnik, M.; Delle Site, L.; Kremer, K. Adaptive resolution scheme for efficient hybrid atomistic-mesoscale molecular dynamics simulations of dense liquids. *Physical Review E* **2006**, *73*, 066701.
 - (76) Fritsch, S.; Poblete, S.; Junghans, C.; Cicciotti, G.; Delle Site, L.; Kremer, K. Adaptive resolution molecular dynamics simulation through coupling to an internal particle reservoir. *Physical review letters* **2012**, *108*, 170602.
 - (77) Delle Site, L.; Praprotnik, M. Molecular systems with open boundaries: Theory and simulation. *Physics Reports* **2017**, *693*, 1–56.
 - (78) Praprotnik, M.; Cortes-Huerto, R.; Potestio, R.; Delle Site, L. Adaptive resolution molecular dynamics technique. *Handbook of materials modeling: methods: theory and modeling* **2018**, 1–15.
 - (79) Krekeler, C.; Agarwal, A.; Junghans, C.; Praprotnik, M.; Delle Site, L. Adaptive resolution molecular dynamics technique: Down to the essential. *The Journal of chemical physics* **2018**, *149*, 024104.
 - (80) Cicciotti, G.; Delle Site, L. The physics of open systems for the simulation of complex molecular environments in soft matter. *Soft matter* **2019**, *15*, 2114–2124.